HHS Public Access

Author manuscript

J Am Chem Soc. Author manuscript; available in PMC 2020 April 24.

Published in final edited form as:

J Am Chem Soc. 2019 April 24; 141(16): 6631–6638. doi:10.1021/jacs.9b01261.

Synthesis of sulfonated carbofluoresceins for voltage imaging

Gloria Ortiz[‡], **Pei Liu**[‡], **Su H. H. Naing**[‡], **Vikram R. Muller**[‡], and **Evan W. Miller**[‡,§,†,*]

[‡] Departments of Chemistry University of California, Berkeley, California 94720, United States.

[§] Departments of Molecular & Cell Biology University of California, Berkeley, California 94720, United States.

[†] Departments of Helen Wills Neuroscience Institute. University of California, Berkeley, California 94720, United States.

Abstract

We present the design, synthesis, and applications of a new class of voltage-sensitive fluorescent indicators built on a modified carbofluorescein scaffold. Carbofluoresceins are an attractive target for responsive probes because they maintain oxygen substitution patterns at the 3’ and 6’ positions, similar to fluorescein, while simultaneously possessing excitation and emission profiles redshifted nearly 50 nm compared to fluorescein. However, the high pK_a of carbofluorescein dyes, coupled with their tendency to cyclize to non-fluorescent configurations precludes their use in voltage-imaging applications. Here, we overcome the limitations of carbofluores-ceins via chlorination to lower the p*K*a by 2 units to 5.2 and sulfonation to prevent cyclization to the non-absorbing form. To achieve this, we devise a synthetic route to halogenated sulfonated carbofluoresceins from readily available, inexpensive starting materials. New, chlorinated sulfone carbofluoresceins have low pK_a values (5.2) and can be incorporated into phenylenevinylene molecular wire scaffolds to create carboVoltage-sensitive Fluorophores (carboVF dyes). The best of the new carboVF dyes, carboVF2.1(OMe).Cl, possesses excitation and emission profiles >560 nm, displays high voltage sensitivity (>30% ΔF/F per 100 mV), and can be used in the presence of other blue-excited fluorophores like green fluorescent protein (GFP). Because carboVF2.1 (OMe).Cl contains a phenolic oxygen, it can be incorporated into fluorogenic labeling strategies. Alkylation with a sterically bulky cyclopropylmethyl-derived acetoxymethyl ether renders carboVF weakly fluorescent; we show that fluorescence can be restored by the action of porcine liver esterase (PLE) both *in vitro* and on the surface of living cells and neurons. Together, these results suggest chlorinated sulfone carbofluoresceins can be promising candidates for hybrid chemical-genetic voltage imaging at wavelengths beyond typical fluorescein excitation and emission.

Table of Contents Graphic

[*]Corresponding Author evanwmiller@berkeley.edu.

ASSOCIATED CONTENT

Supporting Information. Experimental details, synthetic procedures, imaging conditions, and supporting figures. This material is available free of charge via the Internet at http://pubs.acs.org.

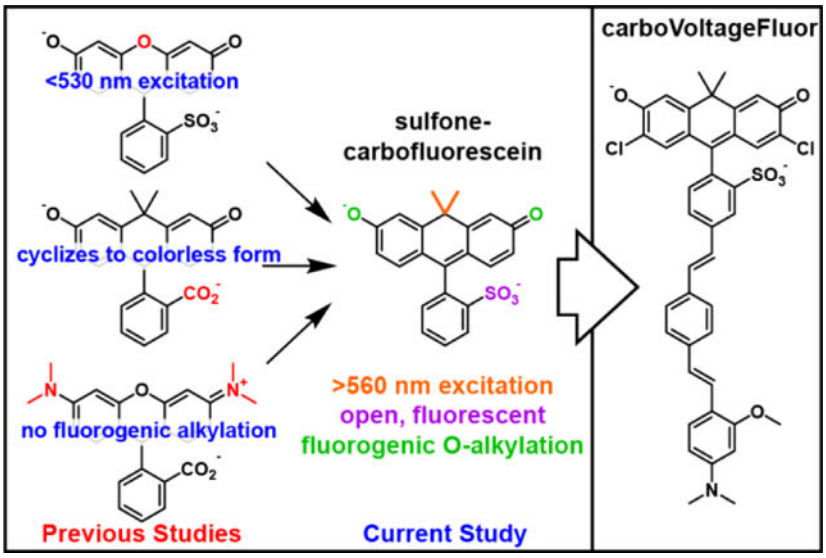

INTRODUCTION

Membrane potential is central to life. Cells exert an array of strategies to maintain tight control over the unequal ionic distribution across their plasma membranes. The millisecond changes in membrane potential associated with electrically excitable cells like neurons and cardiomyocytes are most traditionally studied using electrode-based techniques. While these methods transformed our ability to monitor membrane voltage, they remain low through-put and highly invasive. Optical approaches for measuring membrane voltage dynamics are attractive because they offer the opportunity to probe voltage changes in a minimally-invasive, high-throughput fashion.

Inspired by theoretical descriptions of electron transfer as a voltage-sensing mechanism,[1] coupled with early demonstrations of molecule-scale electric fields altering the efficiency of electron transfer,[2] we recently initiated a program to optically measure membrane voltage in living systems using fluorescent indicators.[3–4] These voltage-sensitive fluorophores, or VoltageFluors, make use of photoinduced electron transfer, or PeT, as a voltage-sensing trigger. Changes in the membrane voltage alter the efficiency of PeT, allowing the fluorescent sensor to toggle between dim and bright states in a voltage-dependent manner. Initial VoltageFluors were based on sulfonefluores- cein[5–7] and provide a fast (sub-microsecond responses)[8–9] and sensitive (>20% ΔF/F per 100 mV) readout of membrane potential. The approach appears generalizable: both rhodamine (RhoVR)[10] and silicon-rhodamine (BeRST)[11] fluorophores can be co-opted to achieve voltage imaging in the >560 nm region of the visible spectrum. The ability to tune voltage sensing across a range of colors enables compatibility with other commonly-used fluorophores, such as the green fluorescent protein (GFP).[12]

A general drawback of chemically-synthesized voltage indicators is their inability to target to specific cells of interest.[13–15] This complicates the interpretation of optical voltage signals, especially in the context of neurobiology, where cell membranes often overlap in the

intricate arborization of neuronal processes. Recently, we showed that fluorescein-based Volt-ageFluors could be ligated directly to cells of interest using self-labeling enzymes like the SpyTag/SpyCatcher system.[16–17] This approach should be generalizable to other colors of voltage-sensitive dye (like RhoVR and BeRST) and to other self-labeling enzymes.[18–21] However, one potential problem is that labeling of cells of interest depends on expression of enzyme on the cell surface. The 1:1 stoichiometry of indicator and enzyme will limit the total number of indicators, and therefore fluorescence intensity, on the cell surface.

The lower fluorescence intensity of the one enzyme, one indicator problem could be partially addressed by fluorogenic approaches in which either photo-uncaging light or cell surface enzyme could catalytically activate the fluorescence of a caged voltage indicator. We showed that both of these strategies, photoactivation and enzymatic uncaging,[22–23] could be employed with fluorescein-based VoltageFluors to provide local contrast and voltage sensing in neurons. This strategy requires the presence of a phenolic oxygen in the fluorophore to enable alkylation-dependent reduction of fluorescence.[24–25] As a result, none of the long-wavelength indicators (>560 nm excitation) developed in our lab, like RhoVR or BeRST can be readily adapted to this fluorogenic strategy, because they rely on rhodamintype xanthenes, which contain substituted nitrogens in place of oxygen at the 3’ and 6’ positions of the xanthene fluorophore (Scheme 1).

We were attracted, therefore, to carbofluorescein-based dyes, which maintain the key phenolic oxygen framework characteristic of fluorescein, but achieve >560 nm excitation and emission by the substitution of the bridge-head oxygen of the xanthene fluorophore with a geminal dimethyl carbon fragment.[26–27] Carbofluorescein scaffolds have been incorporated into PeT- based Ca^{2+} indicators,[28] so we hypothesized that carbofluoresceins could be incorporated into a voltage-sensing platform via installation of a phenylenevinylene molecular wire for membrane localization and voltage sensing. To achieve this, however, would require breaking the propensity for carbofluoresceins to cyclize, in non-polar conditions, to non-absorbing, nonemissive states.[26–27] We hypothesize the open/close equilibrium of carbofluorescein could be shifted to favor the open form by the inclusion of a sulfonate group.

We here report the design, synthesis, and application of a new suite of sulfone-carbofluoresceins to voltage imaging. We established an efficient, 7-step synthesis from readily available, inexpensive starting materials to gain access to novel sulfone-carbofluorescein and halogenated sulfone-carbofluoresceins. All of the new sulfone-carbofluoresceins show a decreased propensity for cyclization and can be combined with phenylene-vinylene molecular wires to yield voltage-sensitive indicators. The best of these, carboVF2.1(OMe).Cl, which is based on a never-before-reported chlorinated carbofluorescein scaffold, shows a voltage sensitivity of 31% ΔF/F per 100 mV in HEK cells with a SNR of 170:1, exceeding that of RhoVR (160:1)[10] and rivaling that of BeRST.[11] We show that carboVF2.1 (OMe).Cl can be adapted to fluorogenic targeting strategies for use in neurons, paving the way for fluorogenic targeting of voltage indicators to specific cells using multiple colors.

RESULTS

Synthesis of sulfone-carbofluorescein dyes

For the application of carbofluoresceins to voltage sensing, a key challenge is the installation of a sulfonic acid group on the *meso* aromatic ring, which we discovered was critical for both preventing passage of molecular-wire fluorescent voltage indicators through cellular membranes[10] and for driving the correct alignment of the voltage-sensing phenylene vinylene molecular wire within the plasma membrane.[4] Sulfone xanthene dyes with oxygen at the 10' bridge-head position, such as fluorescein or rhodamines, can be readily accessed by the acid-catalyzed condensation of the corresponding resorcinols, in the case of fluorescein, or aminophenols, in the case of rhodamines, with carboxylic acids, anhydrides, or aldehydes. Carbofluoresceins and sulfone-carbofluoresceins, where a geminal dimethyl group replaces oxygen at the 10' bridgehead of the xanthene (Scheme 3), cannot be easily synthesized by this analogous route. Previously reported carbofluorescein fluorophores were synthesized through the addition of an aryl-metal species to a protected anthracenyl ketone, yielding unsubstituted carbofluorescein[26] and fluorinated carbofluorescein.[27] We envisioned adapting our earlier synthesis of sulfone silicon-rhodamines[11] to access both unsubstituted and halogenated, sulfone-carbofluoresceins. The short, 6-step synthesis to access reported fluorinated[28] and novel chlorinated ketones **13** and **14** is outlined in Scheme 2. The overall yield for fluorinated ketone **13** is 19%, adding an additional two steps to the previously reported route[27]—with an overall yield of 46%—but beginning with starting materials that are 100-fold less expensive than the starting materials reported in the synthesis of **13**.[27] Additionally, our route provides access, for the first time, to ketone **14** in 14% overall yield, beginning from inexpensive starting materials.

Friedel-Crafts acylation of **2a** or **2b** with *in situ*-generated acid chlorides derived from **1a** or **1b** provides fluorinated benzophenone **3** in 43% yield and the analogous chlorinated benzophenone **4** in 44% yield. Reduction of the ketone with NaBH4 provides benzylic intermediates **5** and **6** in 84% and 80% yield. Intermediates **5** and **6** undergo lithium-halogen exchange mediated by *n*-butyllithium, and treatment with acetone furnishes tertiary alcohols **7** and **8** in 76% and 63% yield. Lewis-acid catalyzed cyclization and simultaneous deprotection of methyl ethers with BBr_3 in CH_2Cl_2 gives anthrone precursors **9** and **10** in 87% and 86% yield. Following column chromatography, these air-sensitive compounds were immediately oxidized with DDQ in a mixture of CH_2Cl_2, dioxane, and water to give **11** and **12**. Subsequent TBS-protection of the alcohols gave the required halogenated, TBS-protected anthrones in 89% (**13**, fluoro) and 88% (14, chloro) yield. Unsubstituted anthrone **15** (X = H, Scheme 3) was prepared according to the reported procedure.[26]

Reaction of aryl lithium species generated from **16** or **17** (R^1 = H or Br) with silyl-protected anthrones **13–15** gave sulfone carbofluorescein dyes **18–23** in yields ranging from 20% to 67%, with halogenated anthrones giving higher yields (> 55%). We found that using the neopentyl sulfonate ester,[29] rather than the corresponding isopropyl ester for **16** and **17**, led to improved yields of sulfone carbofluoresceins (**18–23**). Lithiation of **16** or **17** and addition to the anthrone gave the best results when performed in CH2Cl2 at −20 °C; attempts in THF at a range of temperatures (−78 °C, −40 °C, and −20 °C) gave a complicated mixture of

products or low yields. Sulfone carbofluorescein fluorophores **19**, **21**, and **23** were combined with styrenes **24** or **25** in a Pd-catalyzed Heck reaction to yield carbofluorescein-based voltage indicators **26–31** in 24% to 53% yields after reversephase HPLC purification.

Spectroscopic properties of sulfone carbofluoresceins

Sulfone carbofluoresceins display excitation and emission profiles significantly red-shifted from sulfonated fluoresceins. Sulfone carbofluorescein **18** possesses an absorbance maximum at 550 nm and emission at 576 nm (Fig. 1a,b), while sulfone fluorescein absorbs and emits at 499 and 532 nm.[4] This represents a bathochromic shift of 51 nm and 44 nm for absorption and emission, respectively. This is in good agreement with the 53 and 57 nm shift in absorption and emission observed for traditional fluorescein to carbofluorescein.[26] Sulfonation of carbofluorescein **18** also shifts the absorption and emission profile by 6 and 9 nm, respectively, relative to the parent carbofluorescein (Fig. 1a,b), which absorbs maximally at 544 nm and emits at 567 nm. Again, this is similar to the shift observed when moving from fluorescein to sulfone fluorescein (491 nm to 499 nm for absorption; 510 nm to 532 nm for emission). We observe a similar spectroscopic shift for fluorinated, sulfone carbofluorescein 20 (562/593 nm, abs/em), when compared to the corresponding fluorinated carbofluorescein (555/581 nm, abs/em).[27]

Sulfonation of the *meso* aromatic ring of carbofluorescein derivatives (**18**, **20**, and **22**) results in a drop in the pK_a relative to carboxy-substituted carbofluoresceins. Sulfone carbofluorescein 18 has a p*K*a of 7.11 (± 0.02, Fig. 1c, S1, Table S1), approximately 0.3 log units lower than prototypical carbofluorescein (values ranging from 7.44[26] to 7.54[27]). Fluorine substitution on the 2’ and 7’ positions of sulfone carbofluorescein 20 results in a p*K*a of 5.63 (± 0.02, Fig. 1c, S1, Table S1), a full pH unit lower than 2’,7’-difluorocarbofluorescein without a sulfonate (pK_a = 6.75).[27] Chlorine substitution at the 2’ and 7’ positions further lowers the pK_a of sulfone carbofluorescein **22** to 5.31 ± 0.02 (Fig. 1c, S1, Table S1), compared to 5.0 for dichlorofluorescein.[30] Because halogenated sulfone carbofluoresceins possess pK_a values approximately 1.5–2 units lower than physiological pH, we thought that halogenated sulfone carbofluoresceins would be most useful for cellular imaging, owing to their largely deprotonated and fluorescent state at physiological pH.

A defining characteristic of typical carbofluoresceins is their semi-cooperative transition from a colored, xanthene form to a cyclized and colorless form (Scheme 1), as indicated by Hill coefficients greater than unity for carbofluorescein (1.33 ± 0.03)[26] and fluorinated-carbofluorescein (1.46 ± 0.02).[26] Exchanging carboxylate for sulfonate breaks the cooperativity of carbofluoresceins: both unsubstituted and fluorine-containing, sulfone carbofluoresceins **18** (H) and **20** (F) display Hill coefficients near unity, 0.92 ± 0.01 and 1.02 ± 0.04, respectively. Chlorine-substituted sulfone carbofluorescein **22** (Cl) displays a similar Hill coefficient of 0.99 ± 0.01 (Fig. S1). Sulfonation of the *meso* aromatic ring decreases the propensity of carbofluoresceins to cyclize.

Carbofluorescein VoltageFluors **26–31**, or carboVF dyes, display absorbance and emission profiles similar to their corresponding sulfone carbofluoresceins (**18**, **20**, or **22**, Table 1, Fig. 2a, Fig. S2). The carboVF dyes exhibit lower quantum yields (Table 1) than the

corresponding free fluorophores (Table S1), indicating efficient PeT from the aniline donor to the fluorophore.

Cellular characterization of carbo-VoltageFluor dyes

All of carboVF dyes (26–31) localize to the cellular membranes of HEK293T cells, as determined by fluorescence microscopy (Fig. 2b, Fig. S3). Generally, halogenated carboVFs (**28–31**) display higher cellular brightness than the unhalogenated derivatives (**26** and **27**), likely because the higher pKa of unhalogenated sulfone-carbofluoresceins (7.1 vs 5.6 and 5.3) decreases the fluorescence of unhalogenated carboVFs 26 and 27 at physiological pH. carboVF2.1(OMe).Cl (31) is the brightest dye, with relative fluorescence intensities up to 4-fold greater than carboVF2.1.H (**26**), the dimmest dye, and about 10% brighter than carboVF2.1(OMe).F (**29**) (Table 1, Fig. S3).

All of the carboVF dyes are voltage-sensitive. Patch clamp electrophysiology, coupled with fluorescence imaging, revealed that the carboVF dyes increased fluorescence upon membrane depolarization (more positive potentials) and decreased fluorescence upon hyperpolarization (less positive potentials). When the aniline donor of cVF dyes is unsubsituted (R^2 = H, Scheme 3), carboVF dyes exhibit lower voltage sensitivity (in units of ΔF/F per 100 mV): carboVF2.1.H (**26**) shows a 3% ΔF/F per 100 mV, carboVF2.1.F (**28**) 6%, and car- boVF2.1.Cl (**30**) 7% (Table 1, Fig. S4). The voltage sensitivity of carboVF dyes improves with substitution of the hydrogen on the aniline ring for methoxy (R^2 = OMe), moving to 12% for carboVF2.1 (OMe).H (**27**), 26% for carboVF2.1(OMe).F (**29**), and 31% for carboVF2.1(OMe).Cl (**31**) (Table 1, Fig. 2c,d, Fig. S4). Halogenated carboVF dyes **29** and **31** represent the most sensitive red-shifted, fluorescein-based voltage indicators to date. Dyes with methoxy substitution patterns on the aniline (R^2 = OMe) display higher signal-to-noise ratios (SNR) per 100 mV and show brighter membrane-associated fluorescence in HEK cells—perhaps due to more efficient incorporation into cell membranes. Because of its low pK_a (~5.3), high voltage sensitivity (31% ΔF/F per 100 mV), favorable brightness, and high SNR for detecting voltage changes in cells (~170:1), we carried carboVF2.1(OMe).Cl (31) forward for further characterization in neurons.

CarboVF2.1(OMe).Cl stains membranes of hippocampal neurons cultured from rat embryos and responds to spontaneous neuronal activity with clear, distinct action potentials (Fig. 3a,b). Optical recordings reveal recurrent, spontaneous activity in cultured hippocampal neurons, with action potentials and spiking events from multiple, neighboring cells (Fig. 3c,d). Field stimulation of neurons indicate that carboVF2.1(OMe).Cl responds to action potentials with 14% ± 1% ΔF/F (SNR = 28:1, n = 17 cells, Fig. S5): an improvement over sulfone-fluores-cein-based VoltageFluor2.1.Cl (7.5%, SNR = 20:1)[23] and rho-damine-based RhoVR (9.5%, SNR = 12:1)[10] and comparable to the performance of far-red silicon-rhodamine BeRST (18%).[11]

Fluorogenic targeting of carboVF dyes

Localization of synthetic voltage indicators to specific cells of interest remains an outstanding challenge.[13–14, 17, 21–23, 31] The long-wavelength excitation and emission profile, high voltage sensitivity, ability to report on action potentials in mammalian neurons,

and carbofluorescein molecular scaffold of carboVF derivatives make them an attractive choice for fluorogenic, cell-specific targeting strategies. We previously showed that fluorescein-based VoltageFluor dyes can be adapted to cell-specific targeting through a fluorogenic approach: alkylation of the phenolic oxygen of VF2.1.Cl with either a photolabile nitrobenzyl protecting group[22] or a hydrolytically-stable cyclopropylmethyl acetoxy methyl ether[23] results in decreased fluorescence, which can be restored by photo-uncaging or the action of an exogenously expressed esterase.[32] Localization of porcine liver esterase (PLE) on the cell surface results in VF fluorescence restricted to cells that express PLE.

We hypothesized that combining esterase-mediated targeting with long-wavelength, phenol-containing, or fluorescein-like fluorophores, as opposed to aniline-containing, or rhodamine-like fluorophores, would provide an opportunity for imaging voltage dynamics from specific neurons using longer wavelengths of light. To accomplish this, we synthesized carbo-VoltageFluors targeted by esterase expression (carboVF-EX, Scheme 4). Current voltage-sensitive fluorophore scaffolds with excitation and emission profiles above 560 nm, like RhoVR (rhodamine) or BeRST (silicon-rhodamine) cannot be fluorogenically targeted using these strategies, because they lack the phenolic oxygen present in VoltageFluor and carboVoltageFluor dyes.

CarboVF-EX 1 and 2 are synthesized in a single step from carboVF2.1(OMe).Cl (Scheme 4). Addition of stoichiometric (EX 1) or excess (EX 2) iodo-1-methylcyclopropane-carbox ylate in DMF using N,N-diisopropylethylamine as a base provides the singly and doubly protected carboVF-EX derivatives. Alkylation results in a hypsochromatic shift in the absorption spectrum, from a maximum at 550 nm for carboVF2.1 (OMe).Cl to 420 nm for carboVF-EX 1 (Fig. 4a,b, Fig. S6). Alkylation of the phenolic oxygen of carboVF2.1(OMe).Cl results in a 12-fold decrease in fluorescence quantum yield (Table S2).

The carboVF-EX dyes are substrates for purified PLE (Sigma, E2884). CarboVF-EX1 and EX2 are hydrolyzed by PLE, resulting in a 45- or 21- fold increase in fluorescence, respectively, after 2h. Release of the caged species results in carboVF2.1(OMe).Cl-like absorbance and emission profiles (Fig. 4a,b). HPLC analysis reveals carboVF2.1 (OMe).Cl as the product of PLE-mediated hydrolysis reactions (Fig. S7). Both carboVF-EX 1 and 2 show saturation-type enzymatic kinetics with PLE (Table S2, Fig. 4c, Fig. S6). The Michaelis constant, K_M, for carboVF-EX 1 is 6.4 ± 1 μM and 0.16 ± 0.06 μM for carboVF-EX 2. These values correspond reasonably well with the values we obtained for the fluorescein-based VF-EX 1 (1.2 ± 0.5 μM) and VF-EX 2 (0.12 ± 0.03 μM). All of these values are within the range for the reaction of bis(cyclopropy-lacetoxymethy)-fluorescem, 0.5 μM.[32] The double-protected carboVF-EX 2 is a better substrate for PLE than the singly-protected carboVF-EX 1: the k_{cat}/K_M for carboVF-EX 2 is 4.9×10^5 $M^{-1}s^{-1}$, nearly 5-fold larger than the value for carboVF-EX 1 (1.3×10^5 $M^{-1}s^{-1}$). Again, the measured k_{cat}/K_M values for car- boVF-EX dyes closely match the values obtained for fluorescein VF-EX dyes (Table S2).

Cellular performance of carboVF-EX 1

We next sought to determine if we could elicit a similar turnon phenomenon in living cells. CarboVF-EX 1 (500 nM, 30 min or 1 h) was bath applied to HEK cells transfected with cell-sur-face PLE anchored via a glycophosphatidyl inositol, GPI, anchor (GPI sequence derived from decay-accelerating factor, DAF; Fig. S8).[33] CarboVF-EX 1 was uncaged by PLE on the cell surface, displaying membrane-associated fluorescence in transfected cells (as indicated by nuclear-localized GFP fluorescence, Fig. 5a–c). CarboVF-EX2 did not elicit a turn-on response when bath-applied to PLE-expressing HEK cells (data not shown). We hypothesize that due to the extra carbon dimethyl group ($C(CH_3)_2$), carboVF-EX 2 is more lipophilic than VF-EX2 and does not properly load into cell membranes. Due to these results, we carried carboVF-EX 1 forward in our studies.

HEK cells expressing PLE-DAF and stained with carboVF- EX 1 show a 8.9 (±0.7) and 5.0 (±0.4) fold turn-on after 30 mins and 1 h, respectively, when compared to non-transfected cells from the same culture (Fig. 5a–c, Fig. S9). These results match the observed 7-fold increase in fluorescence after uncaging of VF-EX 1 in HEK cells.[23] As with fluorescein-based VF-EX 1, longer incubation times with carboVF-EX 1 increases the overall fluorescence associated with carboVF-EX 1 in PLE-expressing cells, but decreases the contrast due to accumulation of uncaged carboVF-EX 1 in untransfected cells (Fig. S9). Following enzymatic uncaging, carboVF-EX 1 was voltage sensitive in PLE-DAF expressing HEK cells, displaying an 18% ΔF/F per 100 mV, lower than the 31% ΔF/F displayed by carboVF2.1(OMe).Cl (Fig. 5d,e). The lower fractional voltage sensitivity may be a result of increased background staining with carboVF-EX 1 compared to carboVF2.1(OMe).Cl.

We observe selective staining of neurons expressing PLEDAF under the neuron-specific synapsin promoter (Syn) using carboVF-EX 1 (Fig. 5f–h, Fig. S10). Bath-application of carboVF-EX 1 using 500 nM, 1 pM, or 2 pM results in 2.4-, 2.3, and 1.9-fold turn-on after 30 minutes. We also loaded 500 nM carboVF-EX1 for 1 hr, but saw a decrease in contrast with a 1.8-fold turn-on (Fig. S11). Our results are comparable to those obtained with VF-EX1 (1 μM), which exhibits a 4.1-fold turn-on in neurons after 1 hr.[23] The membrane fluorescence associated with carboVF-EX 1 in neurons is voltage-sensitive. CarboVF-EX 1 responds to field stimulation electrode-evoked action potentials with a voltage sensitivity of 8.4% ΔF/F (SNR = 12 ± 0.8, n = 9 cells, Fig. S12) and was able to record spontaneous spiking events in cultured neurons transfected with PLE-DAF (Fig. 5i) - comparable to the values of VF-EX2 / PLE in cultured neurons that we previously reported (7.3 ± 0.8%, SNR = 20 ± 2.7).

DISCUSSION

In summary, we present the design, synthesis, and applications of a new class of sulfone carbofluorescein dyes towards voltage imaging. We show that inclusion of a sulfonic acid functional group prevents the spirocyclization typical of carbo- fluoresceins and develop a concise synthetic route to halogenated carbofluorescein precursors starting with readily available, inexpensive starting materials. We incorporate unsubstituted, difluoro-and novel dichloro-substituted sulfone carbofluoresceins into a PeT-based voltage-sensing scaffold and

show that all of the new carboVF dyes are voltage-sensitive in mammalian cells. The best of these, carboVF2.1(OMe).Cl, possesses >30% ΔF/F response to 100 mV depolarizations in HEK cells, has excitation and emission spectra >560 nm, and readily reports on action potentials in mammalian neurons. The use of sulfone carbofluoresceins in the context of voltage sensing enables complementation with a growing toolkit of strategies for fluorogenic targeting.[22–23] The resulting dye, carboVF-EX1, is the first long-wavelength voltage sensitive dye targeted to specific cells via enzyme-mediated fluorogenic activation, providing voltage imaging performance rivaling that of previous enzyme-activated voltage indicators, but at long wavelengths compatible with GFP. Future efforts will focus on improving the low contrast ratio between PLE-expressing cells and wildtype cells, by both decreasing the brightness of caged cVF-EXl-type dyes and improving singly-protected cVF-EXl-type dyes as substrates for PLE.

Supplementary Material

Refer to Web version on PubMed Central for supplementary material.

ACKNOWLEDGMENT

Research in the Miller Lab is supported in part by grants from the National Institutes of Health (R35GM119855, R01NS098088), National Science Foundation (NSF 1707350), and the Klingenstein Simons Foundation (40746). GO is a Gilliam Fellow of the Howard Hughes Medical Institute. PL is supported by an A*STAR graduate fellowship. We thank the Francis and Hammond labs for the use of a plate reader and the Catalysis Facility of Lawrence Berkeley National Laboratory, supported by the Director, Office of Science, of the US Department of Energy (contract no. DE-AC02-05CH11231) for the use of the preparative HPLC. We thank Dr. Jeff Pelton for assistance with the 900 MHz NMR spectrometer (NIH P41GM68933).

REFERENCES

1. Li LS, Fluorescence probes for membrane potentials based on mesoscopic electron transfer. Nano Letters 2007, 7, 2981–2986. [PubMed: 17880257]
2. De Silva AP; Gunaratne HQN; Habibjiwan JL; Mccoy CP; Rice TE; Soumillion JP, New Fluorescent Model Compounds for the Study of Photoinduced Electron-Transfer -the Influence of a Molecular Electric-Field in the Excited-State. Angew Chem IntEd 1995, 34 (16), 1728–1731.
3. Miller EW, Small molecule fluorescent voltage indicators for studying membrane potential. Curr Opin Chem Biol 2016, 33, 74–80. [PubMed: 27318561]
4. Kulkarni RU; Yin H; Pourmandi N; James F; Adil MM; Schaffer DV; Wang Y; Miller EW, A Rationally Designed, General Strategy for Membrane Orientation of Photoinduced Electron Transfer-Based Voltage-Sensitive Dyes. ACS Chem Biol 2017, 12 (2), 407–413. [PubMed: 28004909]
5. Orndorff WR; Vose RS, Sulfonefluorescein and dihydroxybenzoyl-benzene-ortho-sulfonic acid, and some of their derivatives. J Am Chem Soc 1924, 46, 1896–1912.
6. Gibbs RC; Shapiro CV, The absorption spectra of sulfonefluorescein and some of its derivatives. J Am Chem Soc 1928, 50 (6), 1755–1762.
7. Jiao GS; Han JW; Burgess K, Syntheses of regioisomerically pure 5- or 6-halogenated fluoresceins. J Org Chem 2003, 68 (21), 8264–7. [PubMed: 14535816]
8. Beier HT; Roth CC; Bixler JN; Sedelnikova AV; Ibey BL, Visualization of Dynamic Sub-microsecond Changes in Membrane Potential. Biophys J 2019, 116 (1), 120–126. [PubMed: 30579565]
9. Miller EW; Lin JY; Frady EP; Steinbach PA; Kristan WB; Tsien RY, Optically monitoring voltage in neurons by photo-induced electron transfer through molecular wires. Proc Natl Acad Sci USA 2012, 109 (6), 2114–2119. [PubMed: 22308458]

10. Deal PE; Kulkarni RU; Al-Abdullatif SH; Miller EW, Isomerically Pure Tetramethylrhodamine Voltage Reporters. J Am Chem Soc 2016, 138 (29), 9085–8. [PubMed: 27428174]
11. Huang YL; Walker AS; Miller EW, A Photostable Silicon Rhodamine Platform for Optical Voltage Sensing. J Am Chem Soc 2015, 137 (33), 10767–76. [PubMed: 26237573]
12. Tsien RY, The green fluorescent protein. Annu Rev Biochem 1998, 67, 509–44. [PubMed: 9759496]
13. Hinner MJ; Hbener G; Fromherz P, Enzyme-induced staining of biomembranes with voltage-sensitive fluorescent dyes. J Phys ChemB 2004, 108 (7), 2445–53.
14. Ng DN; Fromherz P, Genetic targeting of a voltagesensitive dye by enzymatic activation of phosphonooxymethylammonium derivative. ACS Chem Biol 2011, 6 (5), 444–51. [PubMed: 21235276]
15. Kulkarni RU; Vandenberghe M; Thunemann M; James F; Andreassen OA; Djurovic S; Devor A; Miller EW, In Vivo Two-Photon Voltage Imaging with Sulfonated Rhodamine Dyes. ACS Cent Sci 2018, 4 (10), 1371–1378. [PubMed: 30410975]
16. Zakeri B; Fierer JO; Celik E; Chittock EC; Schwarz-Linek U; Moy VT; Howarth M, Peptide tag forming a rapid covalent bond to a protein, through engineering a bacterial adhesin. Proc Natl Acad Sci USA 2012, 109 (12), E690–7. [PubMed: 22366317]
17. Grenier V; Daws BR; Liu P; Miller EW, Spying on Neuronal Membrane Potential with Genetically Targetable Voltage Indicators. J Am Chem Soc 2019, 141 (3), 1349–1358. [PubMed: 30628785]
18. Keppler A; Gendreizig S; Gronemeyer T; Pick H; Vogel H; Johnsson K, A general method for the covalent labeling of fusion proteins with small molecules in vivo. Nat Biotechnol 2003, 21 (1), 86–89. [PubMed: 12469133]
19. Los GV; Encell LP; McDougall MG; Hartzell DD; Karassina N; Zimprich C; Wood MG; Learish R; Ohana RF; Urh M; Simpson D; Mendez J; Zimmerman K; Otto P; Vidugiris G; Zhu J; Darzins A; Klaubert DH; Bulleit RF; Wood KV, HaloTag: a novel protein labeling technology for cell imaging and protein analysis. ACS Chem Biol 2008, 3 (6), 373–82. [PubMed: 18533659]
20. Calloway NT; Choob M; Sanz A; Sheetz MP; Miller LW; Cornish VW, Optimized fluorescent trimethoprim derivatives for in vivo protein labeling. Chembiochem 2007, 8 (7), 767–74. [PubMed: 17378009]
21. Sundukova M; Prifti E; Bucci A; Kirillova K; Serrao J; Reymond L; Umebayashi M; Hovius R; Riezman H; Johnsson K; Heppenstall PA, A Chemogenetic Approach for the Optical Monitoring of Voltage in Neurons. Angew Chem Int Ed 2019, 58 (8), 2341–2344.
22. Grenier V; Walker AS; Miller EW, A Small-Molecule Photoactivatable Optical Sensor of Transmembrane Potential. J Am Chem Soc 2015, 137 (34), 10894–7. [PubMed: 26247778]
23. Liu P; Grenier V; Hong W; Muller VR; Miller EW, Fluorogenic Targeting of Voltage-Sensitive Dyes to Neurons. J Am Chem Soc 2017, 139 (48), 17334–17340. [PubMed: 29154543]
24. Urano Y; Kamiya M; Kanda K; Ueno T; Hirose K; Nagano T, Evolution of fluorescein as a platform for finely tunable fluorescence probes. J Am Chem Soc 2005, 127 (13), 4888–94. [PubMed: 15796553]
25. Kobayashi T; Urano Y; Kamiya M; Ueno T; Kojima H; Nagano T, Highly Activatable and Rapidly Releasable Caged Fluorescein Derivatives. J Am Chem Soc 2007, 129 (21), 6696–6697. [PubMed: 17474746]
26. Grimm JB; Sung AJ; Legant WR; Hulamm P; Matlosz SM; Betzig E; Lavis LD, Carbofluoresceins and carborhodamines as scaffolds for high-contrast fluorogenic probes. ACS Chem Biol 2013, 8 (6), 1303–10. [PubMed: 23557713]
27. Grimm JB; Gruber TD; Ortiz G; Brown TA; Lavis LD, Virginia Orange: A Versatile, Red-Shifted Fluorescein Scaffold for Single- and Dual-Input Fluorogenic Probes. Bioconjug Chem 2016, 27 (2), 474–80. [PubMed: 26636613]
28. Diwu Z; Guo H; Peng R; Zhao Q; Liu J; Liao J Carbofluorescein lactone metal ion indicators and their applications. US20140378344A1, 2014.
29. Miller SC, Profiling Sulfonate Ester Stability: Identification of Complementary Protecting Groups for Sulfonates. J Org Chem 2010, 75 (13), 4632–4635. [PubMed: 20515067]
30. Leonhardt H; Gordon L; Livingston R, Acid-base equilibriums of fluorescein and 2',7'-dichlorofluorescein in their ground and fluorescent states. J Phys Chem 1971, 75 (2), 245–249.

31. Hinner MJ; Hubener G; Fromherz P, Genetic targeting of individual cells with a voltage-sensitive dye through enzymatic activation of membrane binding. Chembiochem 2006, 7 (3), 495–505. [PubMed: 16440375]

32. Tian L; Yang Y; Wysocki LM; Arnold AC; Hu A; Ravichandran B; Sternson SM; Looger LL; Lavis LD, Selective esterase-ester pair for targeting small molecules with cellular specificity. Proc Natl Acad Sci USA 2012, 109 (13), 4756–61. [PubMed: 22411832]

33. Medof ME; Walter EI; Roberts WL; Haas R; Rosenberry TL, Decay accelerating factor of complement is anchored to cells by a C-terminal glycolipid. Biochemistry 1986, 25 (22), 6740–7. [PubMed: 2432921]

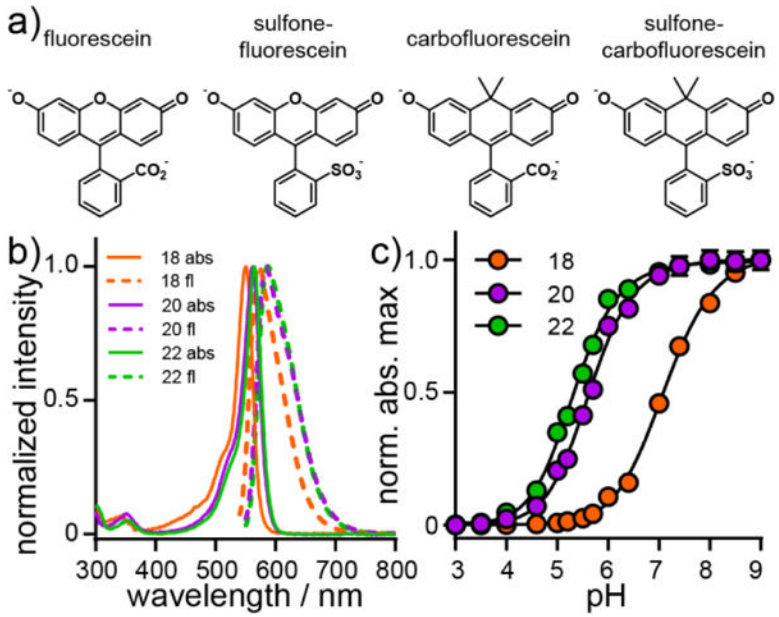

Figure 1.

Spectroscopic characterization of sulfonated carbofluo-resceins. **a**) Structures of sulfonecarbofluorescein and related derivatives. **b**) Plot of normalized absorbance (solid line) and fluorescence emission intensity (dashed line) for **18** (H, orange), **20**, (F, purple), and **22** (Cl, green). Spectra were acquired in HBSS. All dyes were measured at a concentration of 250 nM. **c)** Plot of normalized absorbance maximum vs. pH for **18** (H, orange), **20**, (F, purple), and **22** (Cl, green). Error bars are ± S.E.M. for n = 3 independent determinations. If not visible, error bars are smaller than the marker.

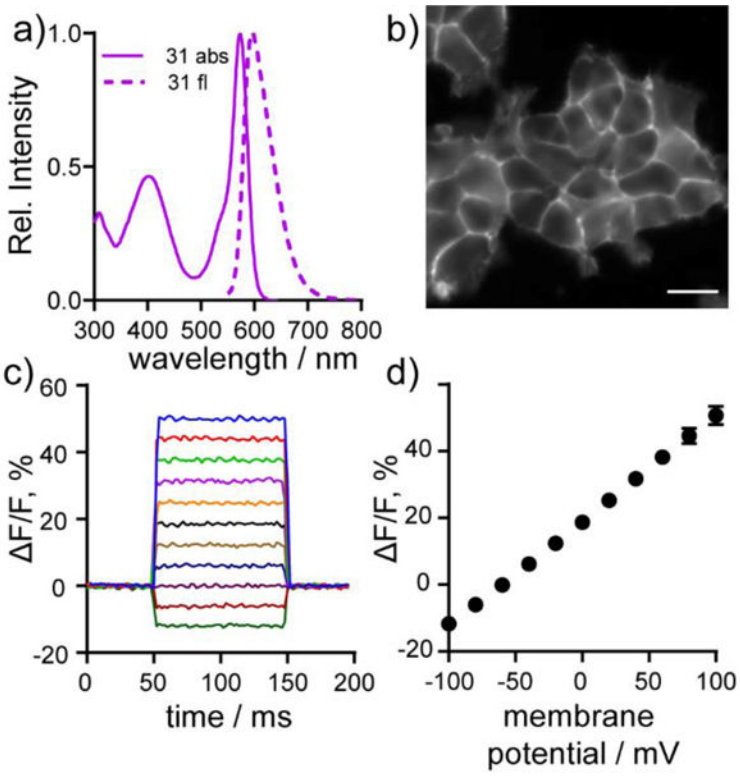

Figure 2.

Cellular and *in vitro* characterization of carbo-VoltageFluor dyes. **a**) Normalized absorbance (solid line) and emission (dashed line) spectra of cVF2.1(OMe).Cl (**31**) in HBSS with 0.01% SDS. **b**) HEK cells stained with 500 nm cVF2.1(OMe).Cl (**31**). Scale bar is 10 μm. c) Plot of the fractional change in fluorescence of cVF2.1(OMe).Cl (**31**) vs time for 100 ms hyper-and depolarizing steps (±100 mV in 20 mV increments) from a holding potential of −60 mV for single HEK cells under whole-cell voltage-clamp mode. (d) Plot of % ΔF/F vs final membrane potential summarizing data from seven separate cells, revealing a voltage sensitivity of approximately 31% per 100 mV. Error bars are ± S.D.

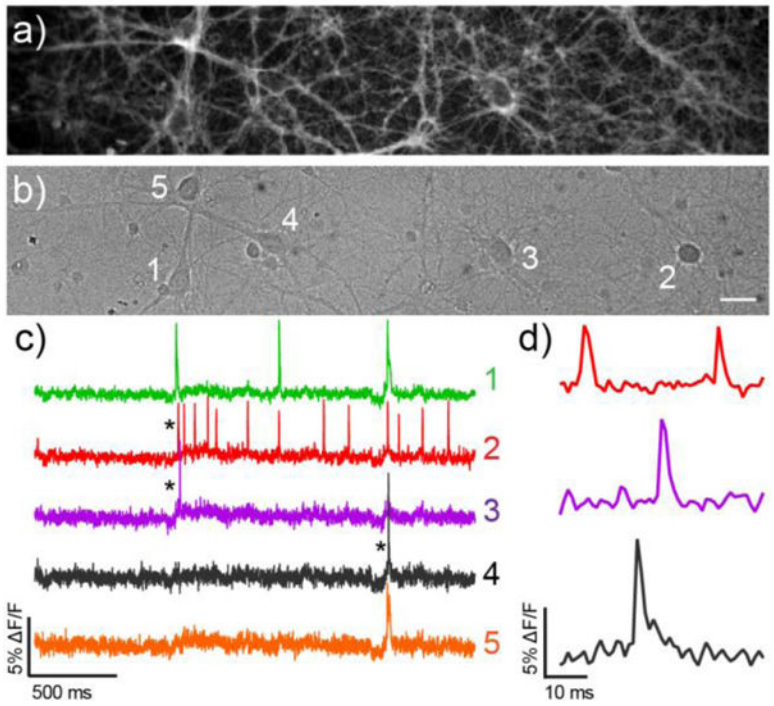

Figure 3.

Voltage Imaging of spontaneous neuronal activity with cVF2.1(OMe).Cl **a**) Fluorescence and **b**) differential interference contrast (DIC) images of cultured rat hippocampal neurons stained with 500 nM cVF2.1(OMe).Cl. Scale bar is 20 μm. **c**) Optical traces of spontaneous activity of the neurons in panels **a–b**) recorded at 500 Hz. Activity is shown as ΔF/F vs time and **d**) shows highlighted and expanded ΔF/F traces.

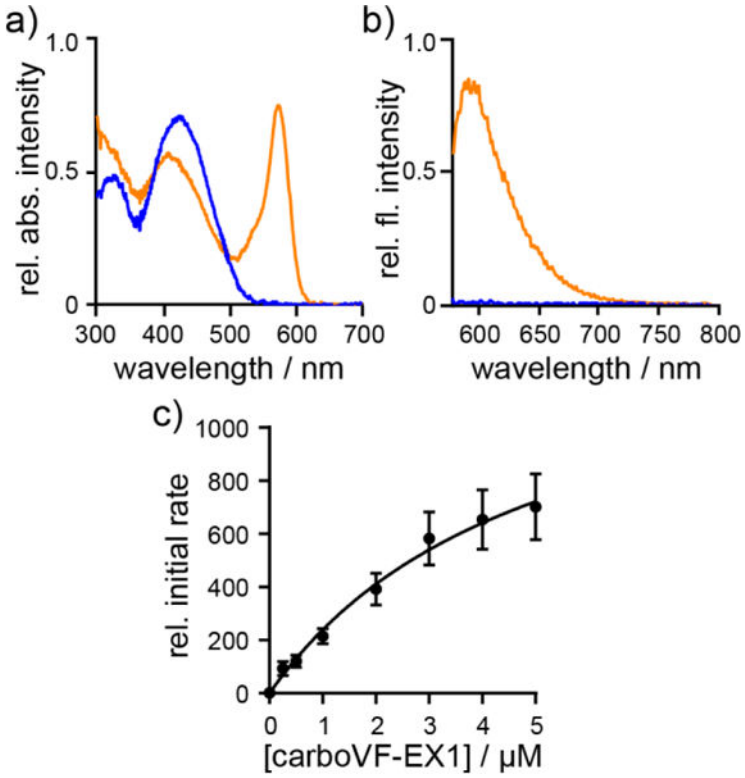

Figure 4.

In vitro characterization of PLE-mediated uncaging of carboVF-EX 1. Normalized **a**) absorbance and **b**) emission spectra of carboVF-EX 1 (0.5 µM) in HBSS with 0.01% SDS. Spectra are acquired 2h after the addition of PLE (0.7 mg/mL, orange) or blank (blue). Excitation is provided at 572 nm. **c**) Plot of relative initial rate vs. carboVF-EX 1 concentration. Error bars are ± S.E.M. for n = 7 independent determinations. [PLE] is 168 ng/mL (1 nM) for saturation kinetics measurements.

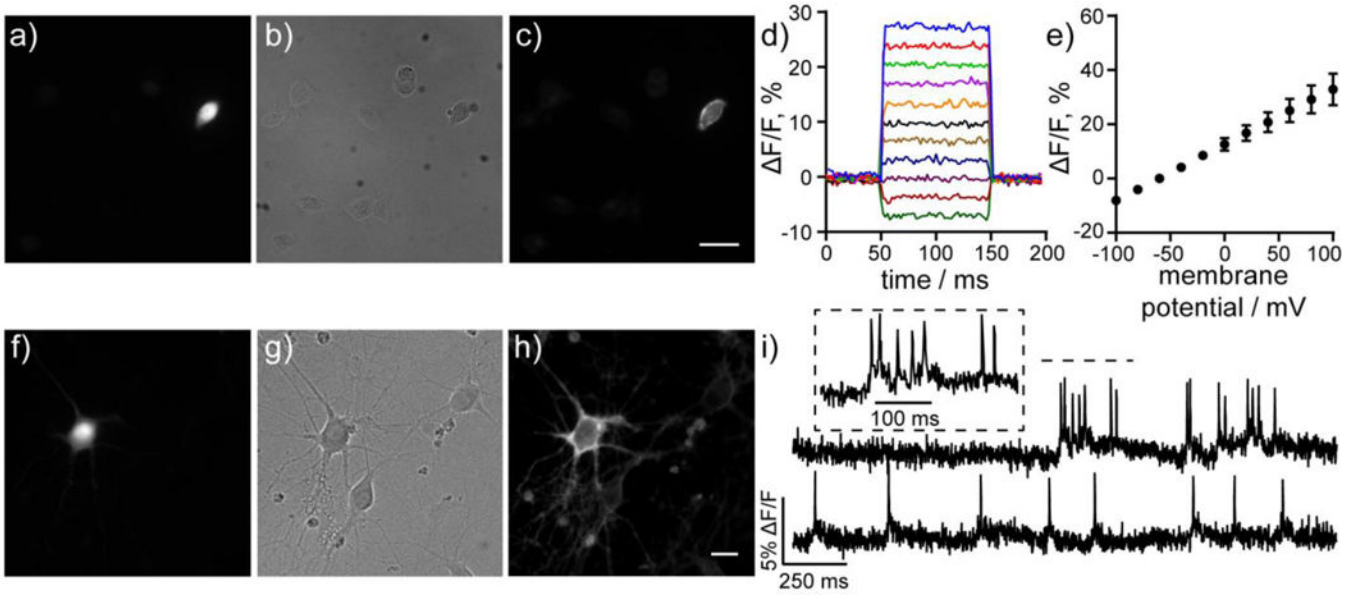

Figure 5.

Cellular characterization of carboVF-EX 1. **a**–**c)** Wide-field fluorescence microscopy of HEK cells stained with carboVF-EX 1 (500 nM, 30 min) shows membrane labeling of the cell expressing cell surface PLE, as indicated by **a**) GFP fluorescence. **b**) DIC image of HEK cells and **c**) epifluorescence image showing carboVF-associated fluorescence in PLE-expressing cell. Scale bar is 10 μm. **d**) Voltage sensitivity of carboVF-EX1 in patch-clamped PLE-expressing HEK cells. **e**) Plot of AF/F vs membrane potential (in mV) for carboVF-EX 1. Data are mean ± S.D. for five cells. **f**–**h**) Live cell wide-field images of rat hippocampal neurons expressing PLE-DAF under the control of the synapsin promoter (Syn) and stained with carboVF-EX 1 (500 nM, 30 min). **f**) GFP fluorescence indicated PLE expression in neurons shown in the **g**) DIC image. **h**) CarboVF-associated fluorescence in PLE expressing neuron. Scale bar is 20 μm. **i**) Representative ΔF/F traces for spontaneous activity of neurons transfected with Syn-PLE and stained with carboVF-EX 1. Images were acquired at 500 Hz and represent single-trial acquisitions. Inset shows expanded time scale of indicated area of the upper trace.

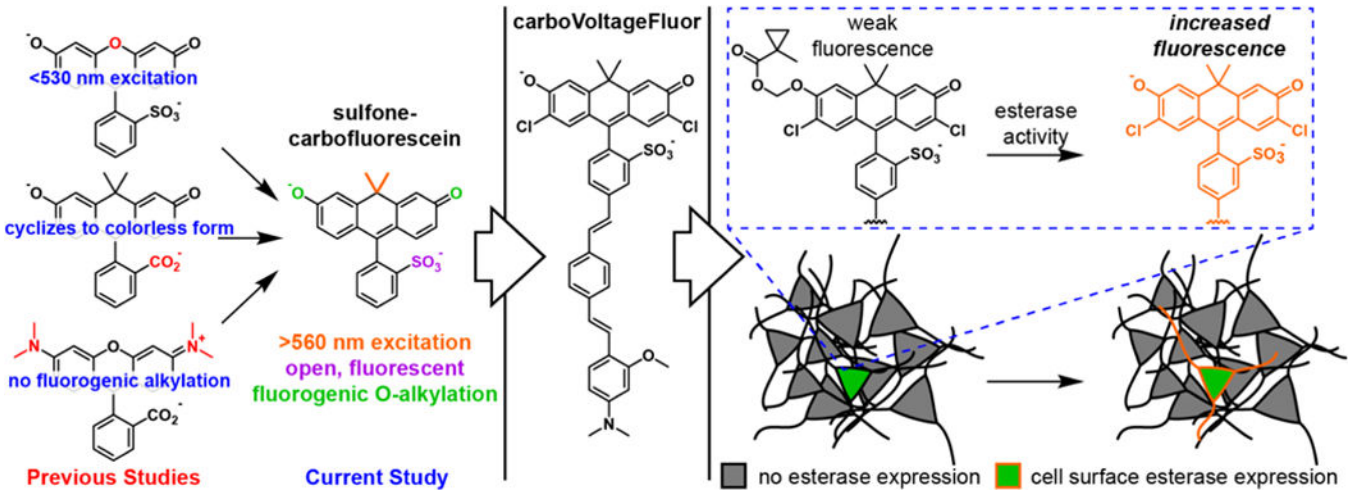

Scheme 1.

Red-shifted voltage-sensitive dyes for fluorogenic targeting to specific cells

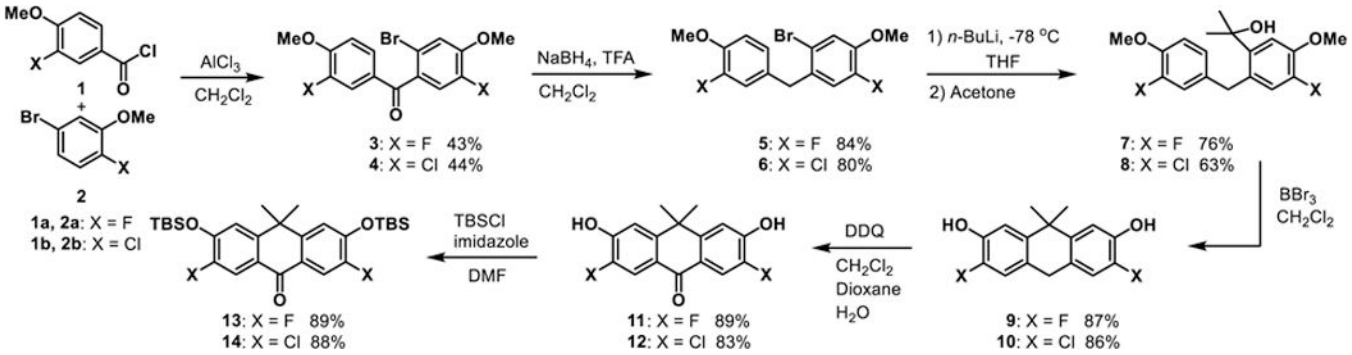

Scheme 2.

Synthesis of carbofluorescein precursors

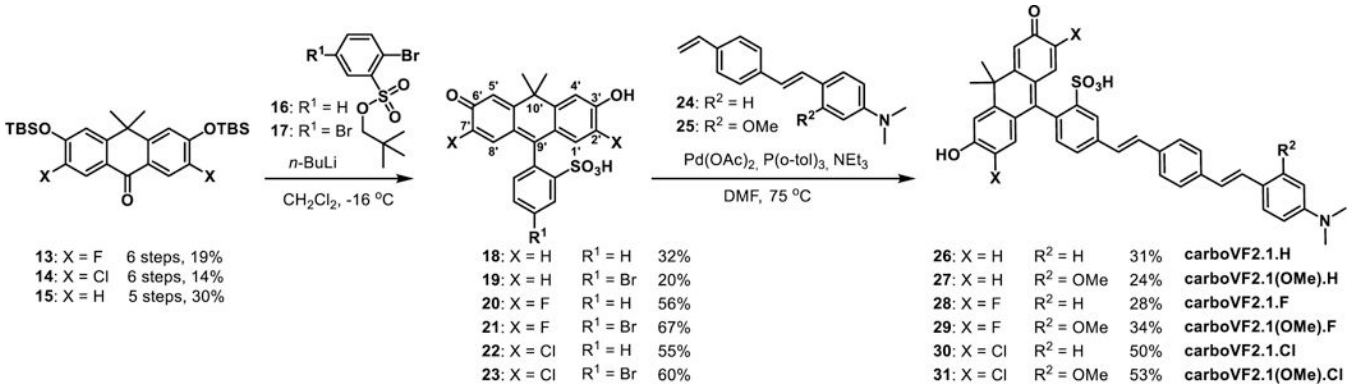

13: X = F 6 steps, 19%
14: X = Cl 6 steps, 14%
15: X = H 5 steps, 30%

18: X = H	R^1 = H	32%	
19: X = H	R^1 = Br	20%	
20: X = F	R^1 = H	56%	
21: X = F	R^1 = Br	67%	
22: X = Cl	R^1 = H	55%	
23: X = Cl	R^1 = Br	60%	

26: X = H	R^2 = H	31%	**carboVF2.1.H**
27: X = H	R^2 = OMe	24%	**carboVF2.1(OMe).H**
28: X = F	R^2 = H	28%	**carboVF2.1.F**
29: X = F	R^2 = OMe	34%	**carboVF2.1(OMe).F**
30: X = Cl	R^2 = H	50%	**carboVF2.1.Cl**
31: X = Cl	R^2 = OMe	53%	**carboVF2.1(OMe).Cl**

Scheme 3.
Synthesis of carboVoltageFluor dyes

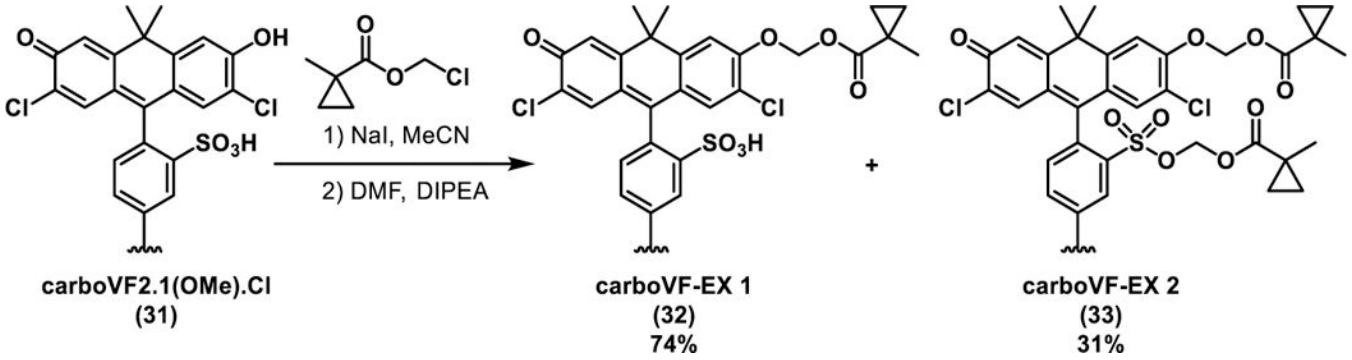

carboVF2.1(OMe).Cl
(31)

carboVF-EX 1
(32)
74%

carboVF-EX 2
(33)
31%

Scheme 4.

Synthesis of carboVoltageFluors targeted by esterse expression, carboVF-EX 1 and 2

Table 1.

Properties of carboVoltageFluor indicators

compound	X	R^2	λmax / nm[a]	λem / nm[a]	Φ[b]	ΔF/F[c,d]	relative brightness[d]	SNR[d,e]
carboVF2.1.H (**26**)	H	H	552	576	0.015	3 ± 1%	0.27 ± 0.03	2.2 ± 0.4
carboVF2.1(OMe).H (**27**)	H	OMe	554	576	0.037	12 ± 1%	0.58 ± 0.07	21 ± 3
carboVF2.1.F (**28**)	F	H	562	593	0.018	6 ± 0.4%	0.84 ± 0.03	19 ± 2
carboVF2.1(OMe).F (**29**)	F	OMe	562	593	0.009	26 ± 2%	0.93 ± 0.04	63 ± 10
carboVF2.1.Cl (**30**)	Cl	H	562	593	0.008	7 ± 1%	0.33 ± 0.01	43 ± 8
carboVF2.1(OMe).Cl (**31**)	Cl	OMe	562	593	0.012	31 ± 2%	1.00 ± 0.05	171 ± 10

[a] Determined in HBSS with 0.01% SDS.

[b] Determined in HBSS.

[c] Per 100 mV.

[d] Determined in HEK cells.

[e] Sampled at 500 Hz. Error is ± S.E.M. for n = at least 5 cells for ΔF/F and SNR determination and n = 3 coverslips (>100 cells per coverslip) for relative brightness.